A Material Law Based on Neural Networks and Homogenization for the Accurate Finite Element Simulation of Laminated Ferromagnetic Cores in the Periodic Regime

Florent Purnode[1], François Henrotte[1], François Caire[2], Joaquim Da Silva[2], Gilles Louppe[1], Christophe Geuzaine[1]
[1]ACE, Institut Montefiore, University of Liège, Belgium - florent.purnode@uliege.be
[2]SKF France

Electromagnetic fields and eddy currents in thin electrical steel laminations are governed by the laws of magnetodynamics with hysteresis. If the lamination is large with respect to its thickness, field and current distributions are accurately resolved by solving a one-dimensional finite element magnetodynamic problem with hysteresis across half the lamination thickness. This 1D model is able to deliver mesoscocpic information to be used, after appropriate homogenization, in the macroscopic modelling of an electrical machine or transformer. As each evaluation of such a homogenised model implies a finite element simulation at the mesoscale, a monolithic coupling might be very time-consuming. This paper proposes an alternative approach, assuming a periodic excitation of the system, where the parameters of a parametric homogenized material law are determined in each finite element with a neural network. The local material law can then be used as a conventional constitutive relationship in a 2D or 3D modelling, with a massive speed-up with respect to the monolithic coupling.

***Index Terms*—Magnetic hysteresis, Magnetic losses, Homogenization, Neural networks.**

I. Introduction

DESPITE an urgent need in industry, there does not yet exist a practical and accurate simulation method to account for magnetic losses in ferromagnetic laminated cores in electrical machine simulations [1]. The detailed analysis of the energy efficiency of electrical machines remains thus a critical open problem, in particular for modern applications with power electronic components switching at higher and higher frequencies [2]. The complexity of this issue is related with the fact that magnetic losses are the macroscopic outcome of the intricate combination of micro or mesoscopic level phenomena : eddy currents, skin effect, saturation and hysteresis. Those phenomena are strongly influenced by both the microstructure of the ferromagnetic material and the laminated structure of the core. Magnetic losses are thus actually determined at geometrical scales much smaller than that of the electrical machine application. An accurate magnetic loss simulation thus requires an explicit modelling of these phenomena, which requires either a fine discretization of all laminations or complex homogenization techniques. In both cases, simulations are extremely costly with days or even weeks of computation, making them impracticable in industrial conception processes [3], [4]. In practice, magnetic losses are usually evaluated a posteriori, based on the induction field computed by the macroscopic electrical machine simulation [5]–[7]. This can however be quite inaccurate. A much more accurate, but still fast, approach based on homogenization and neural networks is presented in this paper. Assuming a periodic excitation of the system, the micro- and mesoscopic phenomena are approximated in the macroscopic model by an irreversible parametric homogenized material law, whose parameters are determined by evaluating a neural network.

II. Parametric Homogenized Material Law

Due to a large aspect ratio, magnetic fields in ferromagnetic laminated cores can be accurately resolved by solving the laws of magnetodynamics with hysteresis over half a lamination thickness [8]. Through homogenization, the solution of this 1D mesoscopic problem is used to identify the irreversible macroscopic law [9]

$$\begin{aligned}\mathbf{H}(\mathbf{B},\dot{\mathbf{B}},p_k) = &\left(p_0 + p_1\left(\frac{|\mathbf{B}|}{\mu^\star H^\star}\right)^{2p_2}\right)\frac{\mathbf{B}}{\mu^\star}\\ &+\left(p_3 + \frac{p_4}{\sqrt{p_5^2+(\frac{|\dot{\mathbf{B}}|}{\mu^\star f^\star H^\star})^2}}\right)\frac{\dot{\mathbf{B}}}{\mu^\star f^\star}\end{aligned} \tag{1}$$

where $\mathbf{H}$ is the magnetic field, $\mathbf{B}$ the magnetic flux density, $\dot{\mathbf{B}}$ its time derivative, and p_k the parameters to be identified. Some normalization constants $\mu^\star = 1000\ \mu_0$, $H^\star = 1000\ A/m$ and $f^\star = 200\ Hz$ are also introduced to maintain the p_k parameters in a limited range. The law has two terms that represent respectively a reversible and an irreversible part of the magnetic field $\mathbf{H}$. The first term, involving 3 parameters, is a reversible anhysteretic saturation curve. The term with p_3 is a dynamic viscosity-like term accounting for the development of eddy currents in the lamination. The term with a square root, finally, accounts for the fact that the saturation curve is shifted to the right in the $\mathbf{H}-\mathbf{B}$ plane when $\dot{\mathbf{B}}$ is positive, and to the left when $\dot{\mathbf{B}}$ is negative, with a maximum shift equal to the coercive field of the ferromagnetic material.

In general, the p_k parameters are identified so as to match as accurately as possible, e.g., by a mean squared error minimization, the homogenized 1D mesoscopic problem solution computed for a given local field excitation $\mathbf{H}(P,t)$ over one period [9]. Since different elements in a typical macroscopic finite element model undergo different field excitations (compare

$\mathbf{H}(P_1,t)$, $\mathbf{H}(P_2,t)$ and $\mathbf{H}(P_3,t)$ on Fig. 1), the identification should be done repeatedly in every element of the macroscopic problem. This makes a monolithic coupling highly time consuming as the 1D mesoscopic problem has to be solved anew for every element in the mesh.

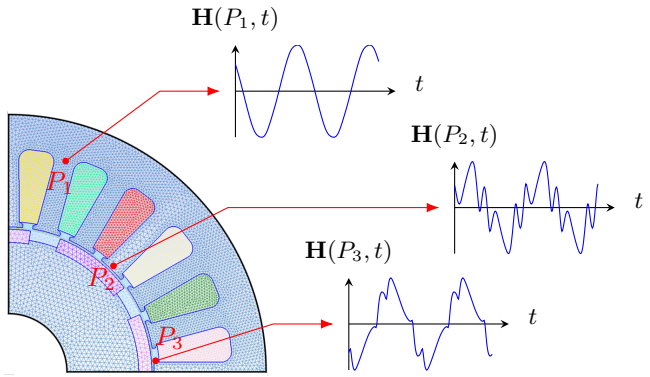

Fig. 1. Mesh of the macroscopic model. Fields vary from one element to the other. Notably, three $\mathbf{H}$ curves are exhibited.

In this paper, this high computational cost is avoided through the use of a neural network specifically trained to realise efficiently and accurately the needed mapping $\mathbf{H}(P,t) \mapsto p_k$.

III. Neural Network

The chosen neural network can be described as a physics-informed auto-encoder. Auto-encoders (see Fig. 2a) are neural networks made up of two parts: the encoder which summarizes the input data and the decoder which reconstructs the input from the encoder summary. In case the decoder accurately reconstructs the input, all the input information is efficiently condensed by the encoder which therefore acts as a feature extractor.

The auto-encoder architecture is implemented by having the encoder predict the p_k values while the $\mathbf{H}(\mathbf{B},\dot{\mathbf{B}},p_k)$ law (1) plays the role of the decoder. The architecture is presented on Fig. 2b and the main training parameters are provided in Tab. I.

To train the neural network, an excitation $\mathbf{H}(t)$ sampled into a sequence of 100 points over a period is given, after min-max normalization, as input to the neural network. This sequence then flows through an embedding network reducing it to a 10-element vector representation of the input. At that level, the main frequency f is concatenated to the sequence. Doing so, rather than adding the frequency to the 100 item long input sequence, gives f more weight in the learning process. The encoder network returns p_k values which are injected into the $\mathbf{H}(\mathbf{B},\dot{\mathbf{B}},p_k)$ function together with the sequences $\mathbf{B}$ and $\dot{\mathbf{B}}$. This returns an estimation $\hat{\mathbf{H}}$ and the mean squared error between $\mathbf{H}$ and $\hat{\mathbf{H}}$ is evaluated and backpropagated.

TABLE I
Parameters of the neural network training.

Batch size:	500	training set:	200 000 sequences
Learning rate:	0.0005	Validation set:	50 000 sequences
Optimizer:	Adam	Test set:	50 000 sequences
Nbr. of epochs:	50 epochs	Learning time:	6 minutes

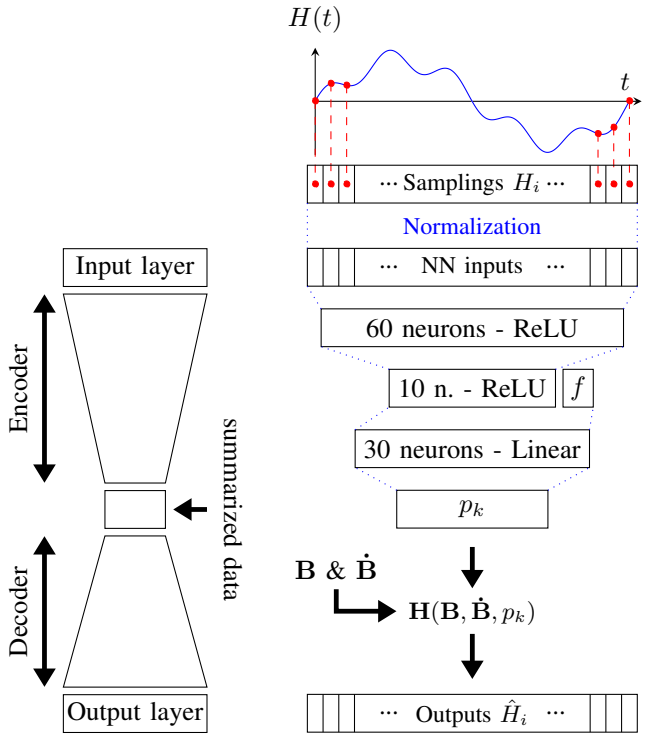

Fig. 2. (a) Auto-encoder architecture. The encoder summarizes the information held at its input. From this summary, the decoder tries to recover the input data. This architecture allows feature extraction. (b) Architecture of the neural network. From a sequence $\mathbf{H}$ and its frequency f, the neural network predicts some p_k values which are injected in the parametric homogenized material law (1) together with the sequences $\mathbf{B}$ and $\dot{\mathbf{B}}$ corresponding to the input sequence $\mathbf{H}$. The law 1 returns an estimation $\hat{\mathbf{H}}$ of the input sequence $\mathbf{H}$. This neural network can be seen as an auto-encoder where the encoder is a simple multilayer perceptron, the summarized data is the p_k values, and the decoder is the parametric homogenized material law (1).

IV. Dataset Generation

In order to train the neural network, a large dataset is generated. This dataset is composed of sequences $\mathbf{H}(t)$ with a sampling rate of 100 points per period. Scalar sinusoidal excitations with at most one harmonic are considered to be representative of the excitation sequences encountered during the macro simulation:

$$H(t) = H_0 \sin(2\pi f_0 t) + \chi H_1 \sin(2\pi f_1 t + \varphi). \qquad (2)$$

The parameters values used in (2) to generate the training dataset are drawn stochastically. The notations $\mathcal{U}$ and $\mathcal{U}_\mathcal{N}$ express uniform distributions respectively over real and integer numbers: $\mathbb{P}(\chi = 1) = 80\,\%$ and $\mathbb{P}(\chi = 0) = 20\,\%$ to consider one or no harmonic, $H_0 \sim \mathcal{U}(100, 2000)$, $f_0 \sim \mathcal{U}(50, 500)$, $f_1 = \alpha f_0$ with $\alpha \sim \mathcal{U}_\mathcal{N}(2, 14)$, $H_1 = \beta H_0$ with $\beta \sim \mathcal{U}(0, \frac{1}{\sqrt{f_1}})$ and $\varphi \sim \mathcal{U}(0, 2\pi)$. The dataset is completed with the corresponding sequences $\mathbf{B}$, obtained by solving the 1D mesoscopic problem with a M23535A 10 electrical steel lamination on the one hand, and with the sequences $\dot{\mathbf{B}}$ obtained by centered differentiation of the latters on the other hand.

V. Numerical Results

In this section, the accuracy and computation time are compared for the identification of the p_k parameters by mean squared error minimization or by using the neural network. In both cases, the error with the homogenized solution H_i, $i = 1, \dots, 100$, of the 1D mesoscopic problem is given by:

$$\text{error} = \sqrt{\frac{\sum_{i=1}^{100} (\hat{H}_i - H_i)^2}{\sum_{i=1}^{100} H_i^2}}. \tag{3}$$

The mean error evaluated on the test set is similar with both approaches. It is evaluated at 19.9% when using the neural network and at 20% with the mean squared error minimisation.

Fig. 3 displays the results obtained with the three excitation sequences $\mathbf{H}(P_i, t)$ depicted in Fig. 1. It notably shows, by comparing the reversible anhysteretic curve with the other three curves, how poor the conventional modelling of ferromagnetic cores with a non-conduction saturable material is compared to a modelling with an irreversible material law like (1).

On the other hand, the neural network approach yields an impressive gain in computation time. On an `i7-9750H` CPU, using `pytorch v1.9.0` and considering one sequence, the neural network p_k prediction and the evaluation of $\mathbf{H}(\mathbf{B}, \dot{\mathbf{B}}, p_k)$ take about 0.5 ms altogether whereas, in the same conditions, the 1D mesoscopic problem resolution takes about 2 seconds. A speed-up of more than three orders of magnitude is thus obtained. This speed-up gets even higher when considering a higher number of sequences, since multiple sequences can be handled at once by the neural network. For instance, the neural network and the $\mathbf{H}(\mathbf{B}, \dot{\mathbf{B}}, p_k)$ evaluations of 10 000 sequences is performed in 34 ms.

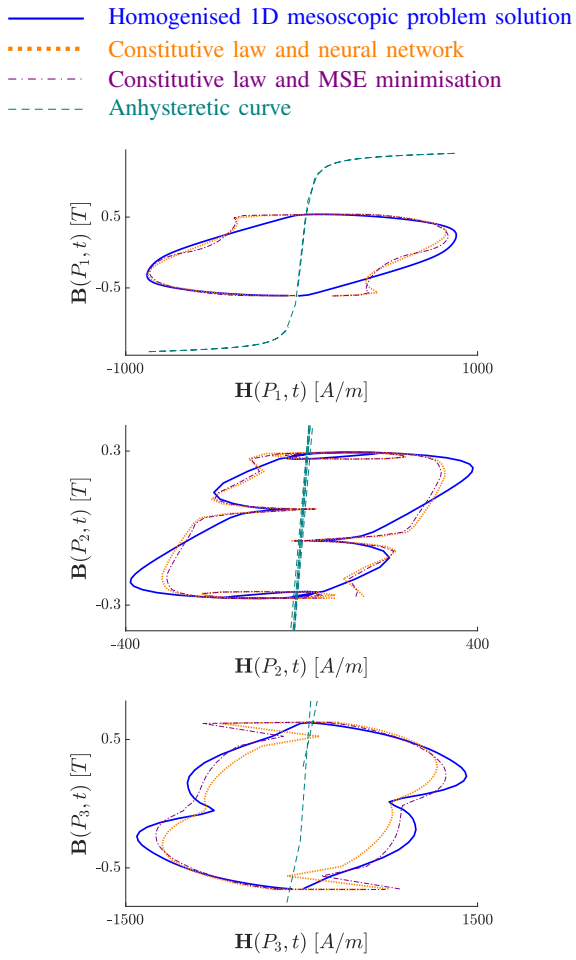

Fig. 3. Response of the different models to the excitation sequences presented in Fig. 1 with the neural network or by mean squared minimization. The homogenized 1D mesoscopic problem solution is the reference. The neural network provides an important speed-up and similar results as the mean squared minimization. In both cases, the prediction is far more accurate than the conventional modelling.

VI. Improved Material Law

One has observed in the previous section that the neural network approach and mean squared error minimization return similar errors. Furthermore, increasing the neural network capacity does not lead to any significant improvement. The main limitation thus originates from the $\mathbf{H}(\mathbf{B}, \dot{\mathbf{B}}, p_k)$ law (1), which probably over-constrains the problem. Further improvements could be obtained by modifying this law.

The terms to add can be assessed by using one-input-one-output neural networks. These neural networks can be seen as high-capacity-parametric one-variable functions that can be learned during the training of the global system. Once the training is achieved, these functions are approximated analytically and the analytical expressions are added as new terms in the law. This procedure led to the following modification of the law (1):

$$\begin{aligned}\mathbf{H}(\mathbf{B}, \dot{\mathbf{B}}, p_k) = &\left(p_0 + p_1 \left(\frac{|\mathbf{B}|}{\mu^\star H^\star} \right)^{2p_2} \right) \frac{\mathbf{B}}{\mu^\star} \\ &+ \left(p_3 + \frac{p_4}{\sqrt{p_5^2 + (\frac{|\dot{\mathbf{B}}|}{\mu^\star f^\star H^\star})^2}} \right) \frac{\dot{\mathbf{B}}}{\mu^\star f^\star}) \\ &+ p_6 \left(\frac{\mathbf{B}}{\mu^\star} \right) \left| \frac{\dot{\mathbf{B}}}{\mu^\star H^\star f^\star} \right|.\end{aligned} \tag{4}$$

With this modified law, the error drops down to 9.5% with the neural network, and to 10.3% with the mean squared error minimisation. Fig. 4 displays the improved responses to the three excitation sequences of Fig. 1. To conclude, Fig. 5 presents the distribution of the p_k parameters and of the error in function of the parameters H_0 (between 100 and 2000 A/m) and $f0$ (between 50 and 500 Hz) in (2), holding $\chi = 1$, $H_1 = H_0/4$, $f_1 = 5f_0$ and $\varphi = 0$ constant. It is observed that the identified parameters depend smoothly on the excitation field $\mathbf{H}(t)$, and that expected features related to, e.g., magnetic saturation show clearly and consistently.

VII. Conclusions

Hysteresis and eddy currents in ferromagnetic laminations can be modelled with an irreversible parametric material law. A mapping relating the material law parameter values with the local field excitations is needed to avoid performing repeatedly the time-consuming identification process. This paper has shown that a specifically trained neural network can realise

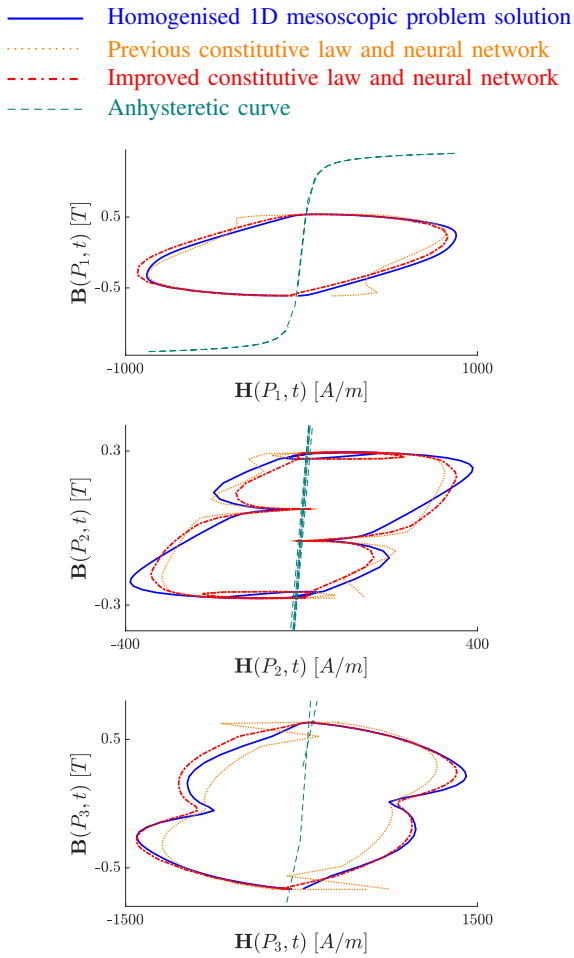

Fig. 4. Response to the excitation sequences presented in Fig. 1 with the modified material law (4). The error is reduced by a factor 2 compared to the initial law (1).

this mapping with a speed-up of several orders of magnitude and an improved accuracy.

In future work, vector field excitations and the non-periodic regime will be considered. The replacement of the analytic material law by a neural network is also a promising continuation of this work.

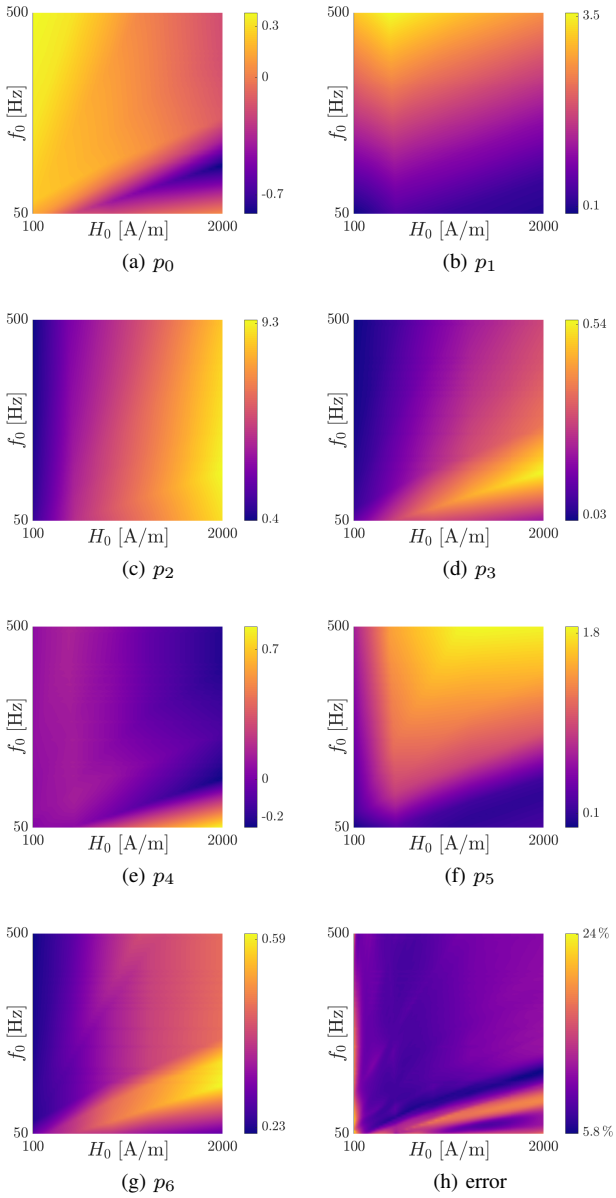

Fig. 5. Neural network mappings of the p_k parameters and of the error considering sinusoidal-with-one-harmonic inputs $H(t) = H_0 \sin(2\pi f_0 t) + \frac{H_0}{4}\sin(2\pi 5 f_0 t)$ on the ranges $H_0 \in [100, 2000]\, A/m$ and $f_0 \in [50, 500]\, Hz$. The identified parameters depend smoothly on the excitation field $\mathbf{H}(t)$.

REFERENCES

[1] E. Dlala, "Comparison of Models for Estimating Magnetic Core Losses in Electrical Machines Using the Finite-ElementMethod", IEEE Transactions on Magnetics, vol. 45, no. 2, pp. 716–725, 2009.

[2] K. Li, P. Evans, M. Johnson, "SiC/GaN power semiconductor devices: a theoretical comparison and experimental evaluation under different switching conditions" IET Electrical Systems in Transportation, 8(1), 3-11, 2018.

[3] I. Niyonzima, R.V. Sabariego, P. Dular, F. Henrotte, C. Geuzaine, "Computational homogenization for laminated ferromagnetic cores in magneto-dynamics", IEEE Trans. Magn., 49, (5), pp. 20492052, 2013.

[4] I. Niyonzima, A. Marteau, G. Meunier, O. Chadebec, N. Galopin, R. Sabariego, C. Geuzaine, "Homogenization of 3D Laminated Cores Using the Heterogeneous Multiscale Method and h-Conforming Formulations", Proceedings of EMF'2021, The 12th International Symposium on Electric and Magnetic Fields, July 2021.

[5] D. Eggers, S. Steentjes, K. Hameyer, "Advanced Iron-Loss Estimation for Nonlinear Material Behavior", IEEE Transactions on Magnetics, vol. 48, no. 11, pp. 3021– 3024, 2012.

[6] G. Von Pfingsten, S. Steentjes, K. Hameyer, "Operating Point Resolved Loss Calculation Approach in Saturated Induction Machines", IEEE Transactions on Industrial Electronics, vol. 64, no. 3, pp. 2538–2546, 2017.

[7] C. Ragusa, C. Appino, F. Fiorillo, "Magnetic losses under two-dimensional flux loci in Fe–Si laminations", Journal of Magnetism and Magnetic Materials, vol. 316, no. 2, pp. 454–457, 2007.

[8] S. Steentjes, F. Henrotte, C. Geuzaine, K. Hameyer, "A dynamical energy-based hysteresis model for iron loss calculation in laminated cores", Int. J. Numer. Model., 2013, 27, (3), pp. 433–44.

[9] F. Henrotte, S. Steentjes, K. Hameyer, C. Geuzaine, "Pragmatic two-step homogenisation technique for ferromagnetic laminated cores", IET Sci. Meas. Technol., pp. 1–8, doi: 10.1049/iet-smt.2014.0201, July 2014.